Centrality of the XBP1-ERN1 axis in transplacental innate immune training via a microbial-derived immunomodulator

Authors: Kyle T. Mincham[1], Anya C. Jones[1], Marie Bodinier[2], Naomi M. Scott[1], Jean-Francois Lauzon-Joset[1,3], Philip A. Stumbles[1,4], Anthony Bosco[1], Patrick G. Holt[1,5†], Deborah H. Strickland[1†*]

Affiliations:

[1]Telethon Kids Institute, University of Western Australia, Nedlands, Western Australia, Australia.

[2]INRA Pays de la Loire, UR 1268 Biopolymers Interactions Assemblies (BIA) Nantes, Nantes, France.

[3]Centre de recherche de l'Institut de Cardiologie et de Pneumologie de Québec, Université Laval, Québec, Canada.

[4]College of Science, Health, Engineering and Education , Murdoch University, Perth, Western Australia, Australia.

[5]Child Health Research Centre, The University of Queensland, Brisbane, Australia.

[†]Joint senior authors.

[*]Corresponding author. Email: Deb.Strickland@telethonkids.org.au Ph: +61 8 6319 1528 Address: Northern Entrance, Perth Children's Hospital, 15 Hospital Avenue, Nedlands, Western Australia, 6009.

Conflict of interest statement: The authors have declared that no conflict of interest exists.

Abstract

We recently reported that the offspring of mice treated during pregnancy with the microbial-derived immunomodulator OM-85 manifest striking resistance postnatally to allergic airways inflammation. Here we localise the potential treatment target to the fetal cDC progenitor compartment which expands to increase the pool of precursor cells available at birth, enabling accelerated postnatal seeding of the lung mucosal cDC network which is required for maintenance of immunological homeostasis in the airways. These cDC progenitors also display treatment-associated activation of the XBP1-ERN1 signalling axis which promotes tissue survival of cDC, particularly within lungs. Previous studies indicate uniquely rapid turnover of lung cDCs at baseline, with further large-scale acceleration of population dynamics during pathogen/aeroallergen challenge. We suggest that enhanced capacity for XBP1-ERN1-dependent cDC survival within the airway mucosal tissue microenvironment may be a crucial element of the OM-85-mediated transplacental "immune training" process which results in postnatal resistance to airway inflammatory disease.

Introduction

The neonatal period represents a time of high risk for infection-related morbidity/mortality resulting from the combined effects of maturational deficiencies in both anti-microbial defense mechanisms that mediate pathogen recognition and elimination, and in the accompanying regulatory mechanisms required for calibration of these responses to minimise inflammatory damage to host tissues[1, 2]. With respect specifically to the lung tissue microenvironment, a crucial factor governing the kinetics of postnatal acquisition of immune competence is the rate of development of the airway mucosal cDC network which controls local immune surveillance[3, 4].

In addition to increased susceptibility to acute infectious/inflammatory diseases, the seeds for early development of a range of non-communicable diseases exemplified by asthma and aero-allergies, are also frequently sewn during this early window period[5], suggesting that maturational deficiencies in immune function(s) may also be risk factors in this context. There is also compelling evidence that certain environmental exposures can potentially play protective roles in the pathogenesis of these diseases. In particular, epidemiological data derived from studies on traditional farming families in Europe and USA suggest that benign environmental microbial exposures of mothers during pregnancy can influence immune education processes within the fetus, leading to reduced susceptibility to postnatal development of potentially chronic respiratory inflammatory diseases[6, 7]. This capacity for microbial exposures to modulate immune development is consistent with the emerging paradigm of "immune training", whereby exposure to certain classes of microbial stimuli can alter the functional state of innate immune cells, likely occurring at the progenitor level

in the bone marrow[8], leading to optimised immune responsiveness to other unrelated microorganisms[9]. With this in mind, there is growing interest in the concept that immune training can be therapeutically harnessed[10], particularly during prenatal development, to enhance immunocompetence within the offspring[11].

In this regard, we recently reported that oral treatment of pregnant mice with the microbial-derived immunomodulatory agent OM-85 reduces susceptibility of their offspring to the development of Th2-driven allergic airways inflammation, and identified the offspring bone marrow as the primary target for maternal treatment effects[12]. Moreover, myeloid DCs in offspring of OM-85 treated mothers in this model displayed increased capacity to regulate levels of activation in response to acute LPS challenge[12], mirroring earlier findings on the increased immunoregulatory capacity of myeloid cells from human neonates whose mothers were exposed to high microbial burdens during pregnancy[13].

In the study presented here, we sought to identify the mechanisms underlying OM-85-mediated transplacental "immune training", focusing on the fetal bone marrow as a potential target.

Results

To elucidate the mechanisms-of-action of maternal OM-85 treatment, we examined the *in utero* fetal response at gestation day 18.5 (Figure 1A), 2 days prior to expected natural term delivery.

Maternal OM-85 treatment selectively accelerates functional maturation of cDCs in fetal bone marrow

Phenotypic analysis of the fetal bone marrow myeloid compartment using multicolour flow cytometry revealed significant expansion of the total dendritic cell (DC) pool in fetuses from OM-85 treated mothers as compared to equivalent fetuses from untreated mothers (Figure 1B). Further characterisation of the bone marrow DC response demonstrated that this increase was restricted to the conventional DC (cDC) subset as previously described[12], with no parallel changes observed in plasmacytoid DC (pDC) (Figure 1B). These fetal changes mirror our recent observations of increased cDC yields from bone marrow cultures and peripheral lung from the offspring of OM-85-treated mothers in the early postnatal period[1]. We next turned our attention to fetal DC maturation state as determined by surface I-A/I-E expression. As shown in Figure 1C, maternal OM-85 treatment for the last half of gestation enhanced I-A/I-E expression on cDC in fetal bone marrow when compared to fetal bone marrow cDC from untreated mothers. Collectively, these observations suggest that transplacental signals generated at the feto-maternal interface following OM-85 treatment during pregnancy can "train" the developing fetal immune system via accelerating the development of functional competence within the fetal bone marrow cDC compartment.

Expansion of fetal bone marrow myeloid progenitor subsets following maternal OM-85 treatment

Previous studies from our laboratory have additionally identified postnatal expansion of bone marrow myeloid progenitor (MP) cell populations as an effect of maternal treatment with OM-85 during pregnancy[12]. Based on these findings, we hypothesised that the enhanced cDC population within fetal bone marrow following maternal OM-85 treatment

would also be accompanied by concomitant upregulation of upstream MP subsets. Analysis of fetal bone marrow Lin$^-$IL-7Rα^-c-Kit$^+$Sca-1$^-$ MP (Figure 2A), Lin$^-$IL-7Rα^-c-Kit$^+$Sca-1$^-$CD16/32^{hi}CD34$^+$ granulocyte-macrophage progenitor (GMP; Figure 2B) and Lin$^-$IL-7Rα^-c-Kit$^+$Sca-1$^-$CD16/32^{hi}CD34$^+$CX3CR1$^+$Flt-3$^+$ macrophage-dendritic cell progenitor (MDP; Figure 2C) populations demonstrated a total increase in all 3 progenitor subsets within the bone marrow compartment following maternal OM-85 treatment, when compared to fetal bone marrow from untreated mothers. Consistent with the findings in Figure 1B and C, these data provide further evidence that maternal OM-85 treatment selectively modulates the offspring bone marrow myeloid lineage *in utero*, beginning at the early-stage myeloid progenitor level through to the terminal cDC populations which are responsible for seeding peripheral tissues during early postnatal life to provide local DC-mediated immune surveillance.

Maternal OM-85 treatment activates key regulators of the UPR pathway in fetal bone marrow

To gain further insight into the molecular mechanisms underpinning the maternal OM-85-treatment effects, we employed transcriptomic profiling of fetal bone marrow cells. Comparison of the transcriptomic profiles in the two groups indicated that maternal OM-85 treatment resulted in 152 differentially expressed genes (DEG) in fetal bone marrow (119 upregulated, 33 downregulated; Figure 3A, Supplementary Table 1). We then interrogated the DEG for enrichment of biological pathways employing *InnateDB*[14], focusing on the upregulated DEG response given the limited number of downregulated DEG identified. In fetal bone marrow, upregulated DEG were enriched for genes involved in multiple aspects

of protein metabolism, the endoplasmic reticulum (ER) stress response, and the unfolded protein response (UPR; Supplementary Table 2).

Upstream regulator analysis was then performed to identify putative molecular drivers of all observed DEG. The data revealed X-box binding protein 1 (XBP1), a transcription factor central to the UPR[15] and crucial in the development, survival and function of multiple cell types including plasma cells[16], eosinophils[17], natural killer (NK) cells[18], T cell subsets[19] and DCs[20, 21], as the most strongly activated molecular driver within fetal bone marrow associated with maternal OM-85 treatment effects (*P*-value = 3.81×10^{-17}, Z-score = 4.427, Figure 3B; Supplementary Table 3), and consistent with this, its downstream target, the canonical UPR sensor Activating Transcription Factor 6 beta (ATF6β)[22, 23] was upregulated (Supplementary Table 3). Additionally, Endoplasmic Reticulum To Nucleus Signalling 1 (ERN1) was identified as an activated driver gene within the fetal bone marrow following maternal OM-85 treatment (*P*-value = 3.32×10^{-6}, Z-score = 2.156; Figure 3B; Supplementary Table 3). Identification of ERN1 is crucial given that during the ER stress response, this gene encodes the ER stress sensor protein inositol-requiring enzyme 1 (IRE1α), responsible for the unconventional cleavage of a 26 nucleotide fragment from *Xbp1* mRNA, resulting in the generation of the active spliced variant of XBP1 (XBP1s) and enabling it to function as a potent transcription factor within the UPR signalling pathway[23]. Collectively, these findings suggest that activation of the UPR pathway may be a central component of the immune training mechanism induced in fetal bone marrow as a result of maternal OM-85 treatment.

Additional candidate drivers in fetal bone marrow following maternal OM-85 treatment included CD38, IL5, and an array of microRNAs (miR) (Figure 3B; Supplementary Table 3)

recognised principally in the context of cancer-associated functions[24-26]. Of note, miR-149-3p (strongly downregulated in Figure 3B) has been shown to negatively regulate Toll-like receptor (TLR) 4 expression in murine monocytic cells *in vitro*[27] and it is possible that other miRs may have similar (but as yet undefined) innate immune regulatory functions[28]. The relevance of this finding TLR4 upregulation in bone marrow derived myeloid cells in this model merits further investigation. Likewise, the identification of the T-cell activation-associated markers CD38 and IL-5 suggests possible contributions from activated T-cells, and these possibilities will also be addressed in follow up studies.

Upregulation of XBP1s expression is restricted to fetal bone marrow cDC precursors following maternal OM-85 treatment

Finally, to obtain evidence confirming that the activated form of XBP1 was upregulated, we measured expression of the active spliced variant of XBP1 (XBP1s) at the protein level within fetal bone marrow. Using multicolour flow cytometry, we identified significant upregulation of intracellular XBP1s expressing $CD11b^{+}CD11c^{+}$ pre-cDCs within fetal bone marrow following maternal OM-85 treatment (Figure 4A, B). While intracellular XBP1s expression was additionally localised within fetal $CD19^{+}B220^{+}$ B cells, $NKp46^{+}CD11b^{+}B220^{+}CD11c^{lo}$ NK cells and $CD3^{+}$ T cells (Supplementary Figure 1), as previously described in the literature[16, 18, 19, 29], maternal OM-85 treatment had no impact on expression levels in these cell types.

Discussion

In this study, we have characterised the response of the fetal bone marrow myeloid cell compartment to maternal treatment with the microbial-derived innate immune modulator OM-85 during pregnancy. We demonstrate that, consistent with our previous reports in 6-

week-old offspring[12], maternal OM-85 treatment expanded the baseline pool of GMP and MDP in fetal bone marrow. Furthermore, maternal OM-85 treatment selectively amplified the overall abundance of fetal bone marrow cDC which are directly downstream of these progenitor subsets, along with enhancing the concomitant functional maturation of these cDC as demonstrated by upregulated I-A/I-E (MHC Class II) expression. This bone marrow population is the source of the precursors which subsequently seed the airway mucosal DC network that progressively develops between birth and weaning[3, 4]. It is noteworthy that the cDC which initially seed this network postnatally are MHC-II^{low} (reflecting their functionally immature status) relative to the high-level expression seen at later ages[3], and the findings above in fetal cDC from the treated group may collectively explain the accelerated postnatal establishment and the enhanced functional maturation of this network observed in their offspring[12]. This DC network plays an essential "gatekeeper" role in immune surveillance of airway surfaces, and hence in protection against both allergic and infectious diseases in the respiratory tract[30, 31], and its relative paucity and reduced functionality during infancy may be an important contributor to increased susceptibility to these diseases during this life phase.

Earlier studies from our group also identified unique features of the population dynamics of this lung cDC network which distinguishes it from comparable populations in other tissues, notably the exceptionally rapid baseline turnover rate of individual cells within the network, ~85% of which are replaced every 24-36 hours[32], with emigration to draining lymph nodes (bearing samples of locally acquired antigens) balanced by recruitment of replacements from bone marrow. Moreover, once development of functional competence is complete[4], this network develops capability for rapid expansion to up to 5-fold baseline density in the

face of acute challenge with airborne pro-inflammatory irritant, allergenic or microbial stimuli[33], the latter response exhibiting kinetics that rival neutrophils[34, 35]. These unique population dynamics suggests that even at baseline, mechanisms that promote lung cDC survival are likely to play a crucial role in the capacity of the network to perform its immune surveillance functions which require onward migration to downstream lymph nodes and subsequent interaction with T-cells as opposed to antigen presentation *in situ*[30]; moreover during prolonged/severe events exemplified by severe viral infections, the added effects of cDC injury resulting from inflammation-associated ER stress[36] would place further pressure on survival times.

In this regard, our transcriptomic analyses of fetal bone marrow from offspring of OM-85-treated mothers also identified upregulated expression of XBP1, ATF6β and ERN1 (encoding IRE1α), key components of the XBP1-ERN1 signalling axis and critical regulators of the UPR pathway[37] which mitigates the effects of ER stress, and moreover localised upregulated production of active XBP1s protein to cDC precursors. Taken together with recent findings on the role for IRE1α-XBP1 signalling and the downstream transcription factor XBP1s in DC development and function[20, 21], these results suggest a central role for the XBP1-ERN1 signalling axis in this OM-85-mediated immune training process.

In further support of this suggestion, other studies demonstrate a significant reduction in $CD11c^{+}$ cells (mirroring that of our pre-cDC phenotype) within $XBP1^{-/-}$ bone marrow cultures, whilst forced overexpression of XBP1s in $XBP1^{-/-}$ DC precursors conversely rescues and subsequently drives expansion of the DC pool *in vitro*[20]. It is also pertinent to note that the cDC population in the lung mucosa is differentially reliant upon XBP1 expression for survival

at baseline relative to cDC from other tissue sites[36], which may be a direct reflection of the uniquely high turnover rates of cDC within the airway mucosal microenvironment[32].

Methods

Animals

Specific pathogen-free BALB/c mice were purchased from the Animal Resource Centre (Murdoch, Western Australia, Australia). All mice were housed under specific pathogen-free conditions at the Telethon Kids Institute Bioresources Centre.

Time-mated pregnancies

Female BALB/c mice 8-12 weeks of age were time-mated with male BALB/c studs 8-26 weeks of age. Male studs were housed individually with 1-2 females overnight. The detection of a vaginal plug the following morning was designated gestation day (GD) 0.5.

Maternal OM-85 treatment

OM-85 (OM Pharma) is an endotoxin-low lyophilised extract containing a cocktail of TLR ligands derived from 8 major respiratory tract bacterial pathogens (*Haemophilus influenzae, Streptococcus pneumoniae, Streptococcus pyogenes, Streptococcus viridians, Klebsiella pneumoniae, Klebsiella ozaenae, Staphylococcus aureus* and *Neisseria catarrhalis*)[38, 39]. Based on previously optimised dosing concentrations[40, 41], time-mated pregnant BALB/c mice selected at random received daily oral feeding of lyophilised OM-85 reconstituted in phosphate-buffered saline (PBS) to a concentration of 400mg/kg body weight for the second half of gestation (GD9.5 – 17.5). Control pregnant mice were left untreated for the duration

of the study. All maternal treatment was performed with a single batch of OM-85 (batch 1812162).

Tissue collection

Pregnant BALB/c mice were sacrificed 24 hours after the final OM-85 dose at GD18.5. Both horns of the uterus were removed and fetuses sacrificed by decapitation. Fetal hind legs (cleaned of excess tissue) were removed. Fetal hind leg samples for flow cytometry were collected into cold PBS + 0.1% bovine serum albumin (BSA) and stored on ice. Fetal hind leg samples for transcriptomic analysis were collected into RNAlater® stabilisation solution (Ambion). Samples collected into RNAlater® were stored overnight at 4°C, then transferred to 1.5ml Eppendorf tubes (Eppendorf) and frozen at -80°C for future transcriptome profiling. Dead fetuses were excluded from the study.

Single-cell suspension preparation

Fetal hind legs were prepared by mincing with a scalpel followed by enzymatic digestion, as previously detailed[12]. Briefly, minced tissue was resuspended in 10ml GKN + 10% fetal calf serum (FCS; Serana) with collagenase IV (Worthington Biochemical Corp.) and DNase (Sigma-Aldrich) at 37°C under gentle agitation for 60 minutes. Digested cells were filtered through sterile cotton wool columns, centrifuged and resuspended in cold PBS for total cell counts.

Flow cytometry

Fetal bone marrow single-cell suspensions were used for all immunostaining. Panels of monoclonal antibodies were developed to enable phenotypic characterisation of committed myeloid cells: CD3-FITC (BD Bioscience; clone 17A2), CD11b-BV510 (BD Bioscience; clone M1/70), CD11c-BV711 (BD Bioscience; clone HL3), CD19-APC-H7 (BD Bioscience; clone 1D3), Gr-1-Biotin (BD Bioscience; clone RB6-6B2), CD45R/B220-PerCP-Cy5.5 (BD Bioscience; clone RA3-6B2) NKp46-PE-Cy7 (BioLegend; clone 29A1.4), SIRP-α-APC (BioLegend; clone P84), I-A/I-E-BV421 (BioLegend; clone M5/114.15.2), F4/80-BV785 (BioLegend; clone BM8), Viability-AF700 (BD Bioscience), Streptavidin-BV605 (BD Bioscience); hematopoietic stem and progenitor cells: CD2-Biotin (BD Bioscience; clone RM2-5), CD3-Biotin (BD Bioscience; clone 145-2C11), CD4-Biotin (BD Bioscience; clone GK1.5), CD5-Biotin (BD Bioscience; clone 53-7.3), CD8α-Biotin (BD Bioscience; clone 53-6.7), CD19-Biotin (BD Bioscience; clone 1D3), CD45R/B220-Biotin (BD Bioscience; RA3-6B2), Gr-1-Biotin (BD Bioscience; clone RB6-6B2), Ter119-Biotin (BD Bioscience; clone TER-119), CD16/32-PerCP-Cy5.5 (BD Bioscience; clone 2.4G2), CD34-FITC (BD Bioscience; clone RAM34), IL-7Rα-PE-Cy7 (BD Bioscience; clone SB/199), Flt-3-PE (BD Bioscience; clone A2F10.1), c-Kit-APC-Cy7 (BD Bioscience; clone 2B8), Sca-1-BV510 (BD Bioscience; clone D7), CX3CR1-APC (BioLegend; clone SA011F11), NKG2D-BV711 (BD Bioscience; CX5), Viability-AF700 (BD Bioscience), Streptavidin-BV605 (BD Bioscience) and XBP1s-expressing bone marrow cells: CD3-FITC (BD Bioscience; clone 17A2), CD11b-BV510 (BD Bioscience; clone M1/70), CD11c-AF700 (BD Bioscience; clone HL3), CD19-APC-H7 (BD Bioscience; clone 1D3), I-A/I-E-AF647 (BD Bioscience; clone M5/114.15.2), CD45R/B220-PE-CF594 (BD Bioscience; RA3-6B2), Gr-1-Biotin (BD Bioscience; clone RB6-6B2), NKp46-PE-Cy7 (BioLegend; clone 29A1.4), F4/80-BV785 (BioLegend; clone BM8), XBP1s-BV421 (BD Bioscience; clone Q3-695), Streptavidin-BV605 (BD Bioscience). Intracellular staining for XBP1s was performed using an intracellular staining buffer kit

(eBioscience). Data acquisition was performed on a 4-laser LSR Fortessa (BD Bioscience). All samples were kept as individuals and not pooled. Immune cell phenotypic characterisation was performed using FlowJo software (version 10.1, Tree Star). Fluorescence minus one staining controls were used for all panels.

Flow cytometric statistical analyses

Statistical analysis and graphing was performed using GraphPad Prism (GraphPad software; version 7.0a). Statistical significance of $p<0.05$ was considered significant. Unpaired, two-tailed Student's *t*-test or Mann Whitney *U* test were used based on distribution of the data as determined by D'Agostino-Pearson omnibus normality test.

Transcriptome profiling (RNA-Seq)

Tissue preparation, RNA extraction and transcriptome profiling. Fetal bone marrow samples were homogenised using a rotor-star homogeniser (Qiagen) and total RNA extracted via TRIzol (Ambion), followed by clean-up using RNeasy MinElute (Qiagen). RNA integrity was determined using an Agilent 2100 Bioanalyzer (Agilent Technologies; RIN: 10 ± 0 (mean ± SD)). 1µg total RNA (n = 32) was shipped on dry ice to the Australia Genome Research Facility (AGRF) for library preparation (TruSeq Stranded mRNA Library Prep Kit, Illumina) and sequencing (Illumina HiSeq2500, 50-bp singe-end reads, v4 chemistry). The raw sequencing data are available from GEO (accession; GSE140143).

RNA-Seq data analysis

Pre-processing and exploratory data analysis: RNA-Seq data was analysed in the R environment for statistical computing. Sequencing data quality control (QC) was performed with the Bioconductor package Rqc[42]. Sequencing reads were aligned to the reference murine genome (mm10) using Subread and summarised at the gene level using featureCounts[43]. Genes with <500 total counts across the data were removed from the analysis. Sample QC was performed by analysing the distribution of the raw read counts to check for sample outliers using boxplots, relative log-transformed expression (RLE) plots and principal component analysis (PCA), before and after global-scale median normalisation. *Differential expression analysis:* Differentially expressed genes (DEG) were identified employing the *DESeq2* package[44]. *DESeq2* utilises a negative binomial distribution model, with a False Discovery Rate adjusted *P*-value for multiple comparisons. Genes were deemed significant with an adjusted *P*-value < 0.1. *Pathways analysis:* Pathways enrichment analysis was performed using the InnateDB database[14] with Benjamini & Hochberg adjusted *P*-value ≤ 0.05 deemed significant. *Upstream regulator analysis:* Ingenuity Systems Upstream Regulator Analysis[45] was employed to identify putative molecular drives of the DEG patterns. Significance was determined by activation Z-score ≥ 2 and *P*-value of overlap ≤ 0.05.

Study approval

All animal experiments were formally approved by the Telethon Kids Institute Animal Ethics Committee, operating under the guidelines developed by the National Health and Medical Research Council of Australia for the care and use of animals in scientific research.

Acknowledgements

The authors wish to acknowledge the animal technicians at the Telethon Kids Institute Bioresources Centre. This study was funded by the National Health and Medical Research Council of Australia. OM Pharma provided the OM-85 at no cost.

Author contributions

KTM, PGH and DHS designed the study. KTM, MB, NMS and JFLJ performed the experiments. KTM, ACJ, MB and DHS analysed the data. PAS and AB contributed to the project design and discussions on data interpretation. KTM, PAS, PGH and DHS wrote the manuscript. All authors reviewed the final version of the manuscript.

References

1. Levy O. Innate immunity of the newborn: basic mechanisms and clinical correlates. Nat Rev Immunol. 2007;7(5):379-90.
2. Adkins B, Leclerc C, Marshall-Clarke S. Neonatal adaptive immunity comes of age. Nat Rev Immunol. 2004;4(7):553-64.
3. Nelson DJ, McMenamin C, McWilliam AS, Brenan M, Holt PG. Development of the airway intraepithelial dendritic cell network in the rat from class II major histocompatibility (Ia)-negative precursors: differential regulation of Ia expression at different levels of the respiratory tract. J Exp Med. 1994;179(1):203-12.
4. Nelson DJ, Holt PG. Defective regional immunity in the respiratory tract of neonates is attributable to hyporesponsiveness of local dendritic cells to activation signals. J Immunol. 1995;155(7):3517-24.
5. Gollwitzer ES, Marsland BJ. Impact of Early-Life Exposures on Immune Maturation and Susceptibility to Disease. Trends Immunol. 2015;36(11):684-96.

6. von Mutius E, Vercelli D. Farm living: effects on childhood asthma and allergy. Nat Rev Immunol. 2010;10(12):861-8.

7. Ober C, Sperling AI, von Mutius E, Vercelli D. Immune development and environment: lessons from Amish and Hutterite children. Curr Opin Immunol. 2017;48:51-60.

8. Kleinnijenhuis J, et al. Long-lasting effects of BCG vaccination on both heterologous Th1/Th17 responses and innate trained immunity. J Innate Immun. 2014;6(2):152-8.

9. Netea MG, et al. Trained immunity: a program of innate immune memory in health and disease. Science. 2016;352(6284):427-36.

10. Mulder WJM, Ochando J, Joosten LAB, Fayad ZA, Netea MG. Therapeutic targeting of trained immunity. Nat Rev Drug Discov. 2019;18(7):553-66.

11. Holt PG, Strickland DH, Custovic A. Targeting maternal immune function during pregnancy for asthma prevention in offspring: harnessing the “farm effect”? J Allergy Clin Immunol. 2020;*In-press*.

12. Mincham KT, et al. Transplacental immune modulation with a bacterial-derived agent protects against allergic airway inflammation. J Clin Invest. 2018;128(11):4856-69.

13. Lisciandro JG, et al. Neonatal antigen-presenting cells are functionally more quiescent in children born under traditional compared with modern environmental conditions. J Allergy Clin Immunol. 2012;130(5):1167-74.e10.

14. Breuer K, et al. InnateDB: systems biology of innate immunity and beyond-recent updates and continuing curation. Nucleic Acids Res. 2013;41(Database issue):D1228-33.

15. Iwakoshi NN, et al. Plasma cell differentiation and the unfolded protein response intersect at the transcription factor XBP-1. Nat Immunol. 2003;4(4):321-9.

16. Reimold AM, et al. Plasma cell differentiation requires the transcription factor XBP-1. Nature. 2001;412(6844):300-7.

17. Bettigole SE, et al. The transcription factor XBP1 is selectively required for eosinophil differentiation. Nat Immunol. 2015;16(8):829-37.

18. Dong H, et al. The IRE1 endoplasmic reticulum stress sensor activates natural killer cell immunity in part by regulating c-Myc. Nat Immunol. 2019;20(7):865-78.

19. Pramanik J, et al. Genome-wide analyses reveal the IRE1a-XBP1 pathway promotes T helper cell differentiation by resolving secretory stress and accelerating proliferation. Genome Med. 2018;10(1):76.

20. Iwakoshi NN, Pypaert M, Glimcher LH. The transcription factor XBP-1 is essential for the development and survival of dendritic cells. J Exp Med. 2007;204(10):2267-75.

21. Osorio F, et al. The unfolded-protein-response sensor IRE-1alpha regulates the function of CD8alpha+ dendritic cells. Nat Immunol. 2014;15(3):248-57.

22. Yoshida H, et al. Endoplasmic reticulum stress-induced formation of transcription factor complex ERSF including NF-Y (CBF) and activating transcription factors 6alpha and 6beta that activates the mammalian unfolded protein response. Mol Cell Biol. 2001;21(4):1239-48.

23. Yoshida H, Matsui T, Yamamoto A, Okada T, Mori K. XBP1 mRNA is induced by ATF6 and spliced by IRE1 in response to ER stress to produce a highly active transcription factor. Cell. 2001;107(7):881-91.

24. Xia B, et al. Upregulation of miR-874-3p and miR-874-5p inhibits epithelial ovarian cancer malignancy via SIK2. J Biochem Mol Toxicol. 2018;32(8):e22168.

25. Stark MS, et al. The "melanoma-enriched" microRNA miR-4731-5p acts as a tumour suppressor. Oncotarget. 2016;7(31):49677-87.

26. Yang D, Du G, Xu A, Xi X, Li D. Expression of miR-149-3p inhibits proliferation, migration, and invasion of bladder cancer by targeting S100A4. Am J Cancer Res. 2017;7(11):2209-19.

27. Shen W, et al. Repression of Toll-like receptor-4 by microRNA-149-3p is associated with smoking-related COPD. Int J Chron Obstruct Pulmon Dis. 2017;12:705-15.

28. Kirchner B, Pfaffl MW, Dumpler J, von Mutius E, Ege MJ. microRNA in native and processed cow's milk and its implication for the farm milk effect on asthma. J Allergy Clin Immunol. 2016;137(6):1893-5.e13.

29. Todd DJ, et al. XBP1 governs late events in plasma cell differentiation and is not required for antigen-specific memory B cell development. J Exp Med. 2009;206(10):2151-9.

30. Holt PG, Strickland DH, Wikstrom ME, Jahnsen FL. Regulation of immunological homeostasis in the respiratory tract. Nat Rev Immunol. 2008;8(2):142-52.

31. Lambrecht BN, Hammad H. Lung dendritic cells in respiratory viral infection and asthma: from protection to immunopathology. Annu Rev Immunol. 2012;30:243-70.

32. Holt PG, Haining S, Nelson DJ, Sedgwick JD. Origin and steady-state turnover of class II MHC-bearing dendritic cells in the epithelium of the conducting airways. J Immunol. 1994;153(1):256-61.

33. McWilliam AS, et al. Dendritic Cells Are Recruited into the Airway Epithelium during the Inflammatory Response to a Broad Spectrum of Stimuli. J Exp Med. 1996;184(6):2429-32.

34. Jahnsen FL, et al. Accelerated antigen sampling and transport by airway mucosal dendritic cells following inhalation of a bacterial stimulus. J Immunol. 2006;177(9):5861-7.

35. McWilliam AS, Nelson D, Thomas JA, Holt PG. Rapid dendritic cell recruitment is a hallmark of the acute inflammatory response at mucosal surfaces. J Exp Med. 1994;179(4):1331-6.

36. Tavernier SJ, et al. Regulated IRE1-dependent mRNA decay sets the threshold for dendritic cell survival. Nat Cell Biol. 2017;19(6):698-710.

37. Grootjans J, Kaser A, Kaufman RJ, Blumberg RS. The unfolded protein response in immunity and inflammation. Nat Rev Immunol. 2016;16(8):469-84.

38. Razi CH, et al. The immunostimulant OM-85 BV prevents wheezing attacks in preschool children. J Allergy Clin Immunol. 2010;126(4):763-9.

39. Rozy A, Chorostowska-Wynimko J. Bacterial immunostimulants--mechanism of action and clinical application in respiratory diseases. Pneumonol Alergol Pol. 2008;76(5):353-9.

40. Scott NM, et al. Protection against maternal infection-associated fetal growth restriction: proof-of-concept with a microbial-derived immunomodulator. Mucosal Immunol. 2017;10(3):789-801.

41. Strickland DH, et al. Boosting airway T-regulatory cells by gastrointestinal stimulation as a strategy for asthma control. Mucosal Immunol. 2011;4(1):43-52.

42. de Souza W, Carvalho BdS, Lopes-Cendes I. Rqc: A Bioconductor Package for Quality Control of High-Throughput Sequencing Data. Journal of Statistical Software, Code Snippets. 2018;87(2):1-14.

43. Liao Y, Smyth GK, Shi W. The Subread aligner: fast, accurate and scalable read mapping by seed-and-vote. Nucleic Acids Res. 2013;41(10):e108.

44. Love MI, Huber W, Anders S. Moderated estimation of fold change and dispersion for RNA-seq data with DESeq2. Genome Biol. 2014;15(12):550.

45. Krämer A, Green J, Pollard J, Jr., Tugendreich S. Causal analysis approaches in Ingenuity Pathway Analysis. Bioinformatics. 2014;30(4):523-30.

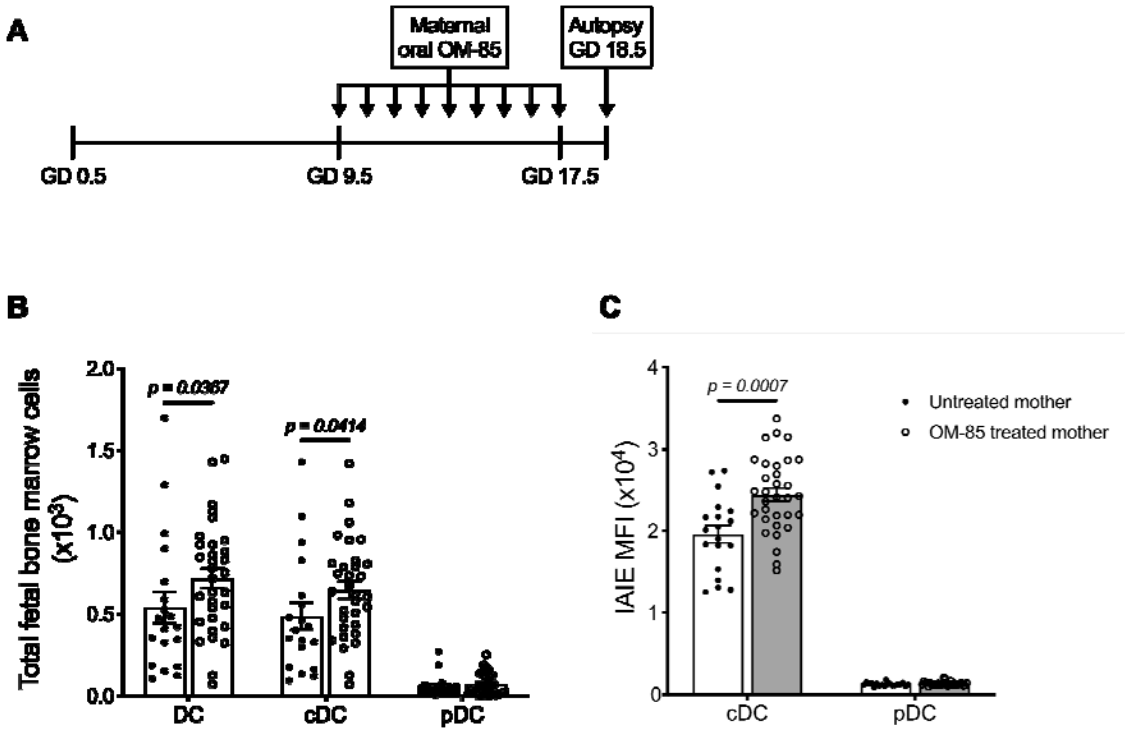

Figure 1. Maternal OM-85 treatment during pregnancy selectively modulates the fetal bone marrow conventional DC subset. (A) Kinetics of maternal OM-85 treatment beginning at gestation day (GD) 9.5 with daily oral treatment until GD 17.5 and autopsy 24 hours post final treatment at GD 18.5. **(B)** Absolute numbers of dendritic cells (DC), $CD11b^{+}B220^{-}CD11c^{+}Gr\text{-}1^{-}SIRP\text{-}\alpha^{+}I\text{-}A/I\text{-}E^{+}$ conventional dendritic cells (cDC) and $CD11b^{-}B220^{+}CD11c^{+}Gr\text{-}1^{+}I\text{-}A/I\text{-}E^{+}$ plasmacytoid dendritic cells (pDC) in fetal bone marrow. **(C)** Mean fluorescence intensity (MFI) of I-A/I-E expression on cDCs and pDCs in fetal bone marrow. Data are presented from individual animals comparing fetuses from OM-85-treated and untreated mothers and displayed as bar graphs showing mean ± SEM of n = 8 independent experiments. Statistical significance was determined using Mann-Whitney U test (B) or Student's t test (C) based on distribution of the data as determined by D'Agostino-Pearson omnibus normality test.

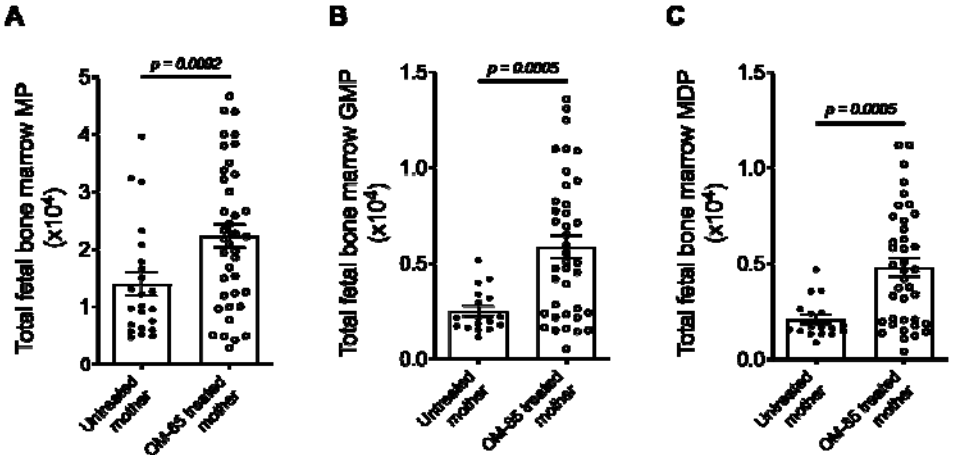

Figure 2. Treatment of mothers with OM-85 during pregnancy boosts myeloid progenitor subsets within fetal bone marrow. Absolute numbers of **(A)** $Lin^{-}IL\text{-}7R\alpha^{-}c\text{-}Kit^{+}Sca\text{-}1^{-}$ myeloid progenitors (MP), **(B)** $Lin^{-}IL\text{-}7R\alpha^{-}c\text{-}Kit^{+}Sca\text{-}1^{-}CD16/32^{hi}CD34^{+}$ granulocyte-macrophage progenitors (GMP) and **(C)** $Lin^{-}IL\text{-}7R\alpha^{-}c\text{-}Kit^{+}Sca\text{-}1^{-}CD16/32^{hi}CD34^{+}CX_{3}CR1^{+}Flt\text{-}3^{+}$ macrophage-dendritic cell progenitors (MDP) in fetal bone marrow. Data are presented from individual animals comparing fetuses from OM-85-treated and untreated mothers and displayed as bar graphs showing mean ± SEM of n = 8 independent experiments. Statistical significance was determined using Student's t test (B) or Mann-Whitney U test (A, C) based on distribution of the data as determined by D'Agostino-Pearson omnibus normality test.

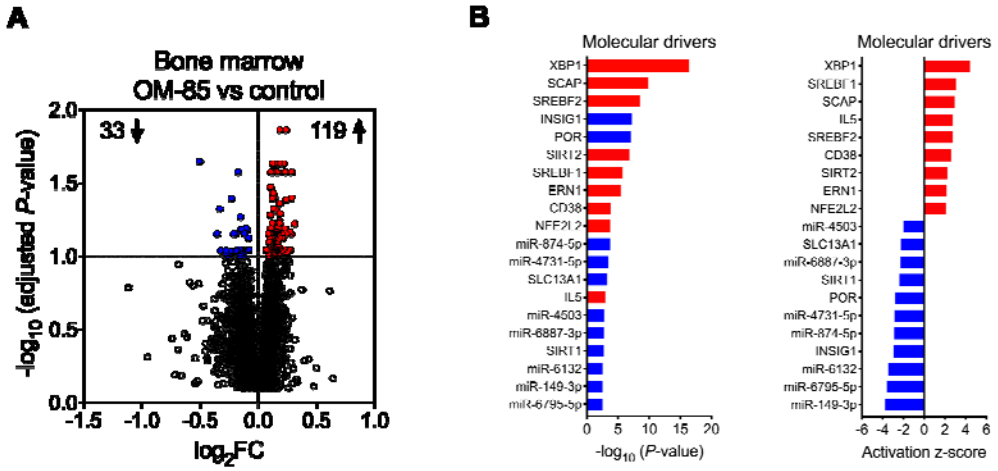

Figure 3. Maternal OM-85-induced changes in fetal bone marrow gene expression profiles. (A) Differentially expressed genes (DEG) within fetal bone marrow comparing offspring from OM-85-treated and untreated mothers. DEG are summarised as volcano plots showing data along axes of statistical significance ($-\log_{10}$ adjusted *P*-value) and differential expression magnitude ($\log_2$ fold change) for n = 16 individual animals per group collected from n = 7 independent experiments. Dashed horizontal lines indicate a False Discovery Rate (FDR) adjusted *P*-value < 0.1. Genes shown in red were upregulated and those shown in blue were downregulated. **(B)** activated (red) and inhibited (blue) molecular drivers of the differential expression patterns were identified using Upstream Regulator Analysis.

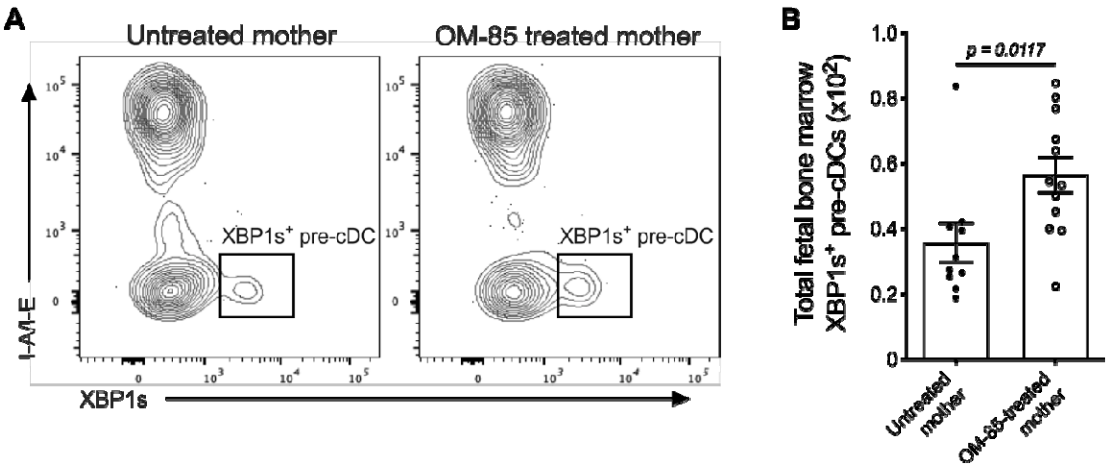

Figure 4. XBP1s expression in pre-cDCs within fetal bone marrow. (A) Representative flow cytometry plots demonstrating intracellular XBP1s expression in $CD11b^{+}B220^{-}CD11c^{+}Gr\text{-}1^{-}I\text{-}A/I\text{-}E^{-}XBP1s^{+}$ pre-conventional dendritic cells (pre-cDCs) within fetal bone marrow. **(B)** Absolute numbers of $XBP1s^{+}$ pre-cDCs in fetal bone marrow. Data are presented from individual animals comparing fetuses from OM-85-treated and untreated mothers and displayed as bar graphs showing mean ± SEM of n = 4 independent experiments. Statistical significance was determined using Mann-Whitney U test.